ChemComm

Accepted Manuscript

This article can be cited before page numbers have been issued, to do this please use: R. A. Rincon, J. Masa, S. Mehrpour, F. Tietz and W. Schuhmann, *Chem. Commun.*, 2014, DOI: 10.1039/C4CC06446A.

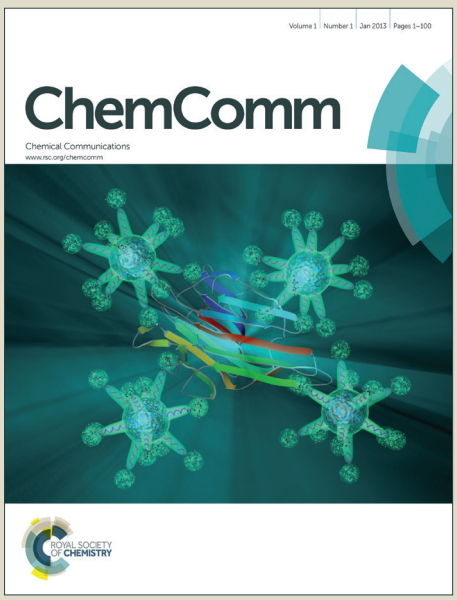

ROYAL SOCIETY OF CHEMISTRY

www.rsc.org/chemcomm

Journal Name

RSCPublishing

View Article Online
DOI: 10.1039/C4CC06446A

COMMUNICATION

Activation of oxygen evolving perovskites for oxygen reduction by functionalization with Fe-N_x/C groups

Cite this: DOI: 10.1039/x0xx00000x

Rosalba A. Rincón,[a] Justus Masa,[a,*] Sara Mehrpour,[a] Frank Tietz,[b] Wolfgang Schuhmann[a,*]

Received 00th January 2012,
Accepted 00th January 2012

DOI: 10.1039/x0xx00000x

www.rsc.org/

The incorporation of Fe-N_x/C moieties into perovskites remarkably activates them for the oxygen reduction reaction (ORR) and also leads to notable improvement of their activity towards the oxygen evolution reaction (OER) thus presenting a new route for realizing high performance, low cost bifunctional catalysts for reversible oxygen electrodes.

The search for low cost catalysts that can catalyze both the oxygen reduction reaction (ORR) and the oxygen evolution reaction (OER) has recently attracted a lot of interest due to their importance in energy conversion and storage technologies including metal-air batteries, electrolyzers and unitized regenerative fuel cell systems. The most active catalysts for both the OER and the ORR are primarily derived from the platinum group metals, which are not only costly but also scarce. Moreover, a major drawback in oxygen electrochemistry is that good catalysts for ORR, such as Pt, are often poor for OER and vice versa, making it very challenging to realize materials that can serve as bifunctional catalysts for both ORR and OER. A strategy that has been used to overcome this impediment is the incorporation of good ORR and OER catalysts into a composite, in which the constituent ORR and OER catalysts retain their individual properties. This strategy has been used in the past with platinum group metals for obtaining bifunctional materials for acid media,[1] and more recently by combining OER active low-cost transition metal oxides with carbon supports that provide ORR functionalities for alkaline media.[2]

Commercial viability of electrochemical devices for energy conversion and storage can only be achieved through the use of low-cost and abundant catalysts. Non-precious metal catalysts derived from pyrolysis of nitrogen rich organic compounds, for example, iron-containing porphyrins or phthalocyanines, and heteroatom-modified carbon materials show the most promising activity towards oxygen reduction.[3,4,5,6] Transition metal oxides with spinel or perovskite type structures show great potential as low-cost alternatives to platinum group metal based oxides for the OER reaction in alkaline media.[7]

In this work, a strategy for realization of non-precious metal bifunctional catalysts was developed, where perovskites with high activity for OER are impregnated with iron phthalocyanine supported on nitrogen-doped carbon and pyrolyzed at 800 °C in an inert gas. We present physico-chemical characterization of the synthesized materials, including electrochemical investigations showing that the resulting catalysts exhibit significantly improved activity for oxygen reduction, while the high OER activity of the perovskites is conserved or even slightly improved in some cases.

Perovskites show promising properties as electrocatalysts for ORR and OER,[8,9] which mainly depend on their composition and stoichiometry. Studies in the literature show that perovskites with the most promising OER activity contain a rare earth or alkaline earth metal like La or Ba occupying the A-site, and transition metals (Co, Fe, Mn, Ni) that allow partial substitution occupying the B-site.[8] For ORR catalysts, activity is reported to be strongly correlated with filling of the δ* orbital (e_g) and the extent of the B-site transition metal-oxygen covalency.[8] To improve the ORR activity of oxygen evolving perovskites, $La_{0.6}Sr_{0.4}FeO_3$, $La_{0.76}Sr_{0.2}Co_{0.2}Fe_{0.8}O_3$, $La_{0.58}Sr_{0.4}Co_{0.2}Fe_{0.8}O_3$ and $La_{0.83}Ca_{0.15}Mn_{0.6}Co_{0.4}O_3$, hereafter denoted as L60SF, L76SCF, L58SCF and LCaMC, respectively, were first impregnated with iron (II) phthalocyanine and nitrogen-doped carbon (NC) in acetonitrile and left to dry under a fume hood. Afterwards, the mixture was pyrolyzed at 800 °C in argon for 2 hours. The pyrolysis of iron-containing nitrogen-rich organic complexes, including porphyrins and phthalocyanines is a well-established method for preparation of active, low cost Fe-N_x/C type catalysts for oxygen reduction.[3,5,6]

Fig. 1 shows SEM images of the L58SCF composite catalyst after the pyrolysis process and grinding. The particles of the perovskite are between 1 and 10 µm (Fig. 1a, also known from particle size distribution)[10] while NC has particles in the 100-300 nm size range (Fig. 1b). Particles of the composite of L58SCF with NC (NC/L58SCF), and also the ones obtained upon incorporation of Fe-N_x moieties (Fe-N_x/C/L58SCF) (Fig. 1c and 1d), range from a few nanometers to several micrometers with NC appearing to cover the perovskite. However, patches existed (Fig. 1d), where the perovskite was clearly exposed, which makes it possible for the composite to retain the OER activity.

Fig. 2 shows the XRD patterns of L58SCF, NC, Fe-N_x/C, NC/L58SCF and Fe-N_x/C/L58SCF. For the pure perovskites, very sharp peaks are present indicating well-crystallized and relatively large-sized particles. For NC and Fe-N_x/C, however, the peaks are very broad due the amorphous small-sized particles. In NC/L58SCF

the characteristic reflections of L58SCF are retained. In addition, the pronounced reflection at 25° from NC merges with that from L58SCF at 23° but they remain distinguishable. The other characteristic reflections of the perovskite remain at their positions, whereas the second reflection of NC and Fe-N_x/C at 43.8° almost disappeared between the reflections of L58SCF at 39.6° and 44.8°. In the diffraction pattern of Fe-N_x/C/L58SC some perovskite reflections shift, and the appearance of new reflections are observed, suggesting some degree of lattice distortion resulting from strong interaction of the perovskite with the Fe-N_x/C moieties.

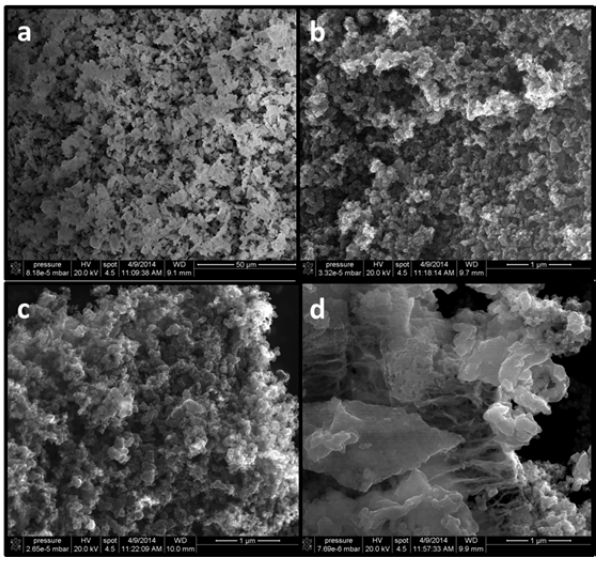

Fig. 1 SEM micrographs of: a) L58SFC, b) NC, c) NC/L58SFC, d) Fe-N_x/C/L58SFC, with EDX spectrum.

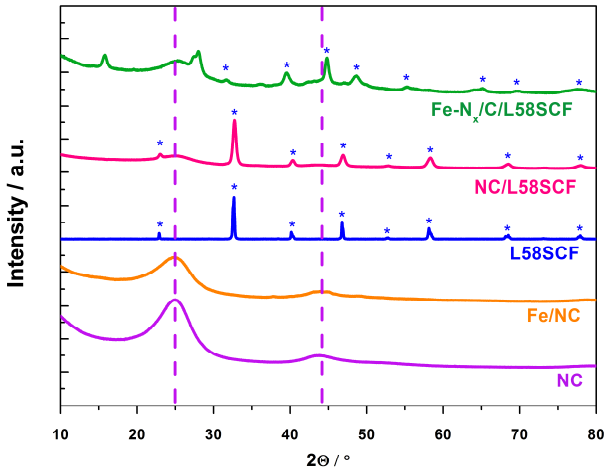

Fig. 2 XRD patterns for samples obtained after different synthesis steps.

Thins films of the catalysts were deposited on glassy carbon rotating disk electrodes (RDE), and their ability to reversibly reduce and evolve oxygen was investigated by recording linear sweep voltammograms (LSV) in oxygen saturated KOH (0.1 M), from 0.0 V to 2.0 V vs RHE at 10 mVs^{-1}, covering the potential range necessary to observe both oxygen reduction and oxygen evolution. We investigated several catalyst loadings, ranging from 75 μg cm^{-2} to 450 μg cm^{-2}, and found 240 μg cm^{-2} to be optimal yielding the highest currents. As shown in Fig. 3a, L58SCF is a good catalyst for OER, but it exhibits very poor ORR activity. The functionalization of this catalyst with NC not only improved its OER activity but also introduced oxygen reduction functionality. The use of NC therefore served two purposes, as a conductive additive to boost the conductivity of the perovskites and as a catalyst for ORR. Conversely, Fe-N_x/C alone is very good for ORR (Fig. 3a) showing a much lower overpotential as compared to L58SCF. However, Fe-N_x/C shows inferior OER activity. It shows a 60 mV overpotential at a current density of 10 mA cm^{-2} as compared to L58SCF. Interestingly, besides the Fe-N_x/C moieties conferring ORR activity to the Fe-N_x/C/L58SCF composite, significant improvement in OER activity is also achieved, reducing the overpotential for OER by 60 mV as compared to L58SCF. Furthermore, the overpotential for ORR is significantly reduced, for example, by 22 mV at a current density of -2 mA cm^{-2} (Fig. 3b).

View Article Online
DOI: 10.1039/C4CC06446A

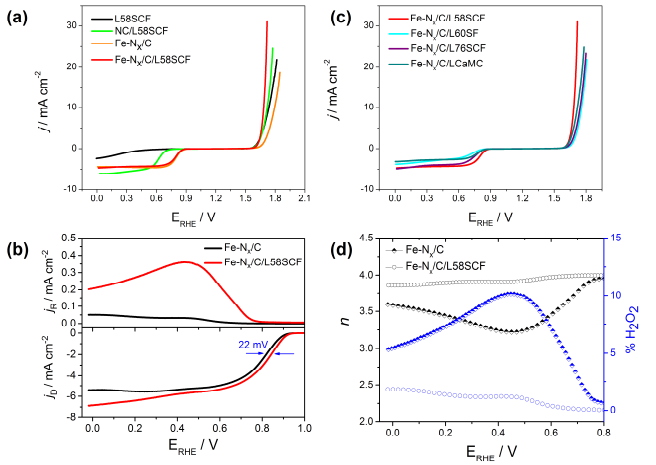

Fig. 3 a) Current response of L58SCF before and after functionalization with NC centers. b) RRDE voltammograms of Fe-N_x/C and Fe-N_x/C/L58SCF recorded at 2500 rpm in O_2-saturated KOH (0.1 M). c) Comparison of the current response of different functionalized perovskites (L58SCF, L60SF, L76SCF and LCaMC); experimental conditions: O_2-saturated KOH (0.1 M), 2500 rpm, 10 mVs^{-1} scan rate. (d) Number of electrons transferred *n* and percentage of H_2O_2 produced during oxygen reduction by Fe-N_x/C and Fe-N_x/C/L58SCF.

Three other perovskites, L60SF, L76SCF and LCaMC, which possess high OER activity but poor ORR activity were also functionalized with Fe-N_x/C moieties in order to test the generality of this approach. Fig. 3c shows a comparison of the four composite materials, where the composite catalyst with L58SFC can be seen to exhibit the highest activity, both for ORR and OER. Table 1 is a summary of the voltage gap between OER and ORR, including the benchmark catalysts for OER (RuO_2 and IrO_2) and ORR (Pt/C), considering the potentials corresponding to currents measured at 10 mA cm^{-2} and -1 mA/cm^{-2} for OER and ORR, respectively. Again, the composite based on L58SCF shows the best bifunctional properties, with a voltage gap of only 0.86 V.

Detailed investigation of the selectivity of the ORR by Fe-N_x/C/L58SCF using RDE voltammetry, and Koutecky-Levich analysis (Fig. S1 in supporting information). The slopes of the Koutecky-Levich plots were; 2.34 at 0.7 V, 2.30 at 0.6 V and 2.28 at 0.5 V, consistent with the theoretical value of 2.27 for a four electron transfer process, as opposed to 4.54 for a two electron transfer process, considering that the diffusion coefficient of O_2 in KOH (0.1 M) is 1.9 x 10^{-5} cm^2 s^{-1}, the Faraday constant is 96485 C mol^{-1}, the

kinematic viscosity of the electrolyte is 0.01 $cm^2 s^{-1}$, the solubility of O_2 in KOH (0.1 M) 1.2 x 10^{-6} mole cm^{-3}.[11] The results thus indicate that the composite catalyst reduces oxygen exclusively to OH^-. This was confirmed by RRDE voltammetry (Fig. 3b) where the percentage of produced H_2O_2 was found to be less than 3.5% (Fig. 3d) at all potentials, whereas Fe-N_x/C alone produced H_2O_2 to up to 10%. To assess the involvement of Fe in constituting the active sites in the Fe-N_x/C/L58SC catalyst, inhibition studies using SCN^- ions were performed, resulting in an increase in the overpotential for ORR and a decline in the electrocatalytic current (Fig. S4), thus confirming that Fe is directly involved in constituting active centers, consistent with results reported by others.[12] The low fraction of H_2O_2 generated by Fe-N_x/C/L58SCF in contrast to Fe-N_x/C also suggests that Fe-N_x/C/L58SCF could be more effective at disproportionating H_2O_2 than Fe-N_x/C.

Table 1. Voltage gap between OER and ORR for synthesized composite materials and commercial catalysts

Catalyst	E_{OER} at 10 mA cm^{-2} / V	E_{ORR} at -1 mA cm^{-2} / V	ΔE ($E_{OER} - E_{ORR}$) / V
RuO_2	1.64	0.54	1.10
IrO_2	1.70	0.38	1.32
Pt/C	2.19	0.97	1.22
L58SCF	1.74	0.29	1.45
NC/L58SCF	1.72	0.67	1.05
Fe-N_x/C	1.80	0.83	0.97
Fe-N_x/C/L58SCF	1.68	0.82	0.86
Fe-N_x/C/L60SF	1.76	0.74	1.02
Fe-N_x/C/L76SCF	1.74	0.79	0.95
Fe-N_x/C/LCaMC	1.72	0.78	0.94

The developed catalyst, Fe-N_x/C/L58SCF shows comparatively stable performance during ORR (Fig. S3a), however, due to accumulation of gas bubbles on the electrode surface during oxygen evolution, which leads to eventual detachment of the catalyst film, gradual loss in performance was observed during OER. Future work will focus on the design of the catalyst films to accelerate gas departure and minimize detachment of the films in order to probe their electrochemical stability.

We have shown that impregnation of perovskites with a nitrogen-rich organic complex containing Fe, in this case iron(II) phthalocyanine followed by pyrolysis, leads to the formation of a highly active bifunctional catalyst for both oxygen reduction and oxygen evolution in KOH (0.1 M). The voltage between ORR at -1 mA cm^{-2} and OER at 10 mA cm^{-2} was as low as 0.86 V, which is remarkably lower than that observed for state-of-the art Pt/C, IrO_2 and RuO_2 catalysts.

Acknowledgement

Financial support by the Helmholtz Association through the "Initiative and Networking Fund" in the framework of the Helmholtz Energie Allianz "Stationäre elektrochemische Feststoff-Speicher und -Wandler" (Contract No.: HA-E-0002) is gratefully acknowledged.

Notes and references

[a] Analytical Chemistry - Center for Electrochemical Sciences (CES), Ruhr-Universität Bochum, Universitätsstr. 150, D-44780 Bochum, Germany. justus.masa@rub.de; wolfgang.schuhmann@rub.de
[b] Forschungszentrum Jülich GmbH, IEK-1, D-52425 Jülich, Germany

View Article Online DOI: 10.1039/C4CC06446A

Electronic Supplementary Information (ESI) available: [details of any supplementary information available should be included here]. See DOI: 10.1039/c000000x/

1 a) G. Chen, S. R. Bare and T. E. Mallouk, *J. Electrochem. Soc.*, 2002, **149**, A1092; b) Y. Zhang, C. Wang, N. Wan and Z. Mao, *Int. J. Hydrogen Energy*, 2007, **32**, 400.

2 a) H. Ohkuma, I. Uechi, N. Imanishi, A. Hirano, Y. Takeda and O. Yamamoto, J. Power Sources, 2013, **223**, 319; b) L. Wang, X. Zhao, Y. Lu, M. Xu, D. Zhang, R. S. Ruoff, K. J. Stevenson and J. B. Goodenough, *J. Electrochem. Soc.*, 2011, **158**, A1379; c) M. de Koninck, S.-C. Poirier and B. Marsan, *J. Electrochem. Soc.*, 2006, **153**, A2103; d) Z. Chen, A. Yu, R. Ahmed, H. Wang, H. Li and Z. Chen, *Electrochim. Acta*, 2012, **69**, 295; e) Y. Liu, D. C. Higgins, J. Wu, M. Fowler and Z. Chen, *Electrochem. Commun*., 2013, **34**, 125–129; f) A. Zhao, J. Masa, W. Xia, A. Maljusch, M. Willinger, G. Clavel, K. Xie, R. Sclögl, W. Schuhmann and M. Muhler, *J. Am. Chem. Soc.* , 2014, **136**, 7551; g) J. Masa, W. Xia, I. Sinev, A. Zhao, Z. Sun, S. Grützke, P. Weide, M. Muhler and W. Schuhmann, *Angew. Chem. Int. Ed*., 2014, **53**, 8508.

3 G. Wu, K. L. More, C. M. Johnston and P. Zelenay, *Science*, 2011, **332**, 443.

4 a) F. Jaouen, E. Proietti, M. Lefèvre, R. Chenitz, J.-P. Dodelet, G. Wu, H. T. Chung, C. M. Johnston and P. Zelenay, *Energy Environ. Sci.*, 2010, **4**, 114; b) Z. Chen, D. Higgins, A. Yu, L. Zhang and J. Zhang, *Energy Environ. Sci.*, 2011, **4**, 3167; c) U. I. Koslowski, I. Abs-Wurmbach, S. Fiechter and P. Bogdanoff, *J. Phys. Chem. C*, 2008, **112**, 15356.

5 M. Lefèvre, E. Proietti, F. Jaouen and J.-P. Dodelet, *Science*, 2009, **324**, 71.

6 K. Kamiya, K. Hashimoto and S. Nakanishi, *Chem. Commun. (Camb.)*, 2012, **48**, 10213.

7 a) W. G. Hardin, J. T. Mefford, D. A. Slanac, B. B. Patel, X. Wang, S. Dai, X. Zhao, R. S. Ruoff, K. P. Johnston and K. J. Stevenson, *Chem. Mater.*, 2014, 140515083621004; b) A. Grimaud, K. J. May, C. E. Carlton, Y.-L. Lee, M. Risch, W. T. Hong, J. Zhou and Y. Shao-Horn, *Nature Commun.*, 2013, **4**; c) J.-I. Jung, H. Y. Jeong, J.-S. Lee, M. G. Kim and J. Cho, *Angew. Chem. Int. Ed.*, 2014, **53**, 4582; d) M. Komo, A. Hagiwara, S. Taminato, M. Hirayama and R. Kanno, *Electrochem.*, 2012, **80**, 834; e) M. Risch, K. A. Stoerzinger, S. Maruyama, W. T. Hong, I. Takeuchi and Y. Shao-Horn, *J. Am. Chem. Soc.*, 2014, **136**, 5229.

8 J. Suntivich, H. A. Gasteiger, N. Yabuuchi, H. Nakanishi, J. B. Goodenough and Y. Shao-Horn, *Nature Chem*, 2011, **3**, 546.

9 J. Suntivich, K. J. May, H. A. Gasteiger, J. B. Goodenough and Y. Shao-Horn, *Science*, 2011, **334**, 1383.

10 R.A. Rincón, E. Ventosa, F. Tietz, J. Masa, S. Seisel, V. Kuznetsov, W. Schuhmann, *ChemPhysChem*. DOI: 10.1002/cphc.201402137.

11 J. Masa, A. Zhao, W. Xia, M. Muhler and W. Schuhmann, *Electrochim. Acta*, 2014, **128**, 271.

12 a) Q. Wang, Z.-Y. Zhou, Y.-J. Lai, Y. You, J.-G. Liu, X.-L. Wu, E. Terefe, C. Chen, L. Song, M. Rauf, N. Tian and S.-G. Sun, *J. Am. Chem. Soc.*, 2014, **136**, 10882; b) J. Masa, A. Zhao, W. Xia, Z. Sun, B. Mei, M. Muhler and W. Schuhmann, *Electrochem. Commun*, **34**, 113; c) W. Li, J. Wu, D. C. Higgins, J.-Y. Choi and Z. Chen, *ACS Catal.*, 2012, **2**, 2761.